

Provided for non-commercial research and education use.
Not for reproduction, distribution or commercial use.



This article appeared in a journal published by Elsevier. The attached copy is furnished to the author for internal non-commercial research and education use, including for instruction at the authors institution and sharing with colleagues.

Other uses, including reproduction and distribution, or selling or licensing copies, or posting to personal, institutional or third party websites are prohibited.

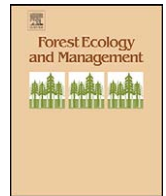
In most cases authors are permitted to post their version of the article (e.g. in Word or Tex form) to their personal website or institutional repository. Authors requiring further information regarding Elsevier's archiving and manuscript policies are encouraged to visit:

<http://www.elsevier.com/copyright>



Contents lists available at ScienceDirect

Forest Ecology and Management

journal homepage: www.elsevier.com/locate/foreco

A hierarchical approach coupled with coarse DEM information for improving the efficiency and accuracy of forest mapping over very rugged terrains

Guopeng Ren^{a,b}, A-Xing Zhu^{c,d}, Wei Wang^a, Wen Xiao^e, Yong Huang^a, Guoqiang Li^e, Depin Li^e, Jianguo Zhu^{a,*}

^a Ecology, Conservation, and Environment Center, Kunming Institute of Zoology, The Chinese Academy of Sciences, 32 Jiaochang Donglu, Kunming, Yunnan, 650223, China

^b Graduate University of Chinese Academy of Sciences, Beijing, 100049, China

^c State Key Laboratory of Resources and Environmental Information Systems, Institute of Geographic Sciences and Natural Resources Research, Chinese Academy of Sciences, Beijing, 100101 China

^d University of Wisconsin-Madison, 550 N Park Street, Madison, WI, 53706, USA

^e Institute of Eastern-Himalaya Biodiversity Research, Dali University, Dali, Yunnan, 671000, China

ARTICLE INFO

Article history:

Received 27 October 2008

Received in revised form 23 March 2009

Accepted 26 March 2009

Keywords:

Forest mapping

Landsat ETM+ image

Steep mountainous terrain

Northwest Yunnan

Digital elevation model

ABSTRACT

Forest mapping over mountainous terrains is difficult because of high relief. Although digital elevation models (DEMs) are often useful to improve mapping accuracy, high quality DEMs are seldom available over large areas, especially in developing countries. In this study, a hierarchical approach coupled with topographic information derived from coarse DEM was developed to improve the efficiency and accuracy of forest mapping over mountainous areas. The overall idea of increasing mapping accuracy over large mountainous areas is to reduce spectral variety over areas to be mapped. The approach consists of three major steps. The first step is to partition a large mountainous area into several small mapping zones. Forest mapping is then conducted in each zone independently. At the second step, forest areas are separated from non-forest areas through a semi-automatic binary classification procedure. At the third step, forested areas are then further classified into detailed forest types by coupling Landsat ETM+ imagery and two topographic variables derived from a coarse DEM (extracted from 1:250,000 digital elevation contour layer, which are readily available). This hierarchical approach was illustrated and evaluated through a case study in Northwest Yunnan, China, a very rugged terrain in the world. Forests and non-forests were separated accurately and efficiently (the overall accuracy is 0.97 and Khat value is 0.94 of whole area). It was found that the inclusion of the coarse topographic data improved the mapping accuracy significantly (overall accuracy from 0.74 to 0.84, from 0.76 to 0.89, from 0.78 to 0.84 in three test areas, respectively), and that the difference in accuracy between the use of coarse DEM data and the use of fine DEM data for the study area is not significant (overall accuracy from 0.84 to 0.86). The results indicate that the hierarchical approach, coupled with coarse DEM information, is effective in increasing the accuracy of forest mapping over very rugged terrains when high quality digital elevation models are not available.

© 2009 Elsevier B.V. All rights reserved.

1. Introduction

Forest maps are required for a variety of ecological applications, such as forest management and wildlife habitat prediction (Skidmore et al., 1996; Osborne et al., 2001; Wulder et al., 2003; Zhu and Waller, 2003). Forest mapping based on Landsat imagery is a cost-efficient means over large areas (> 10,000 km²) (Homer et al., 1997; Cihlar, 2000; Reese et al., 2002; Olthof and Fraser, 2007). However, it is still difficult to map forest in the steep mountainous terrain based on Landsat imagery due to the impact

of high relief (Tokola et al., 2001; Dorren et al., 2003; Blesius and Weirich, 2005).

There remain three challenges for forest mapping over large mountainous terrains, especially in developing countries. First, there are many shadows in the remote sensing imagery due to high relief (Saha et al., 2005). These shadows are hard to be interpreted automatically. Furthermore, the strong topographic variations in mountainous terrain may cause pixels of the same forest cover type to be spectral heterogeneous and pixels of different types to have similar spectral characters (Fahsi et al., 2000). Consequently, the accuracy of forest map produced from an automatic mapping procedure over steep mountainous terrain is often low (Dorren et al., 2003). Visual interpretation of remote sensing images became a possible alternative for mapping forests over areas with

* Corresponding author. Tel.: +86 871 519 0776; fax: +86 871 519 0776.
E-mail address: zhu@mail.kiz.ac.cn (J. Zhu).

high relief (Xiao et al., 2003; Jiang et al., 2004; Kushwaha and Hazarika, 2004; Zemek et al., 2005; Liu et al., 2006). But visual interpretation is very tedious and time-consuming. Second, it is difficult to collect ground truth data through field survey in the mountainous areas due to the poor transportation condition over these areas. Some sites are even inaccessible (Reese et al., 2002). Third, high quality digital elevation models (DEMs), such as these derived from contour maps with a minimum scale of 1:50,000 and these with a resolution of 50 m or better, are seldom available over mountainous areas in developing countries (Richter, 1998; Wechsler, 2003; Paul et al., 2004), although they are proved useful to improve the accuracy of forest mapping based on Landsat images (Frank, 1988; Franklin and Wilson, 1992; Richter, 1998; Fahsi et al., 2000; Dorren et al., 2003).

To overcome these challenges, we present a top-down hierarchical approach coupled with coarse DEM information to map forest over large steep mountainous regions. We will evaluate the effect of a coarse DEM derived from 1:250,000 topographic maps on the accuracy improvement through a case study. In the next section, we will present the method which is followed by a detailed case study in Northwest Yunnan, China. The results of this case study are presented in Section 4. Discussion and summary are presented in Section 5.

2. Methods

The top-down hierarchical classification is a multiple stages process in which broad categories are first separated and finer categories within broad categories are further classified (Townsend and Walsh, 2001). Some classical land cover (including vegetation) classification schemes, such as Anderson system (Anderson et al., 1976), Chinese vegetation schemes (Wu, 1980), and CORINE Land Cover 2000 (Bossard et al., 2000), employ a hierarchical framework to describe variation of vegetation. Thus, it is natural to map land cover using a hierarchical approach to guide classification (Avcı and Akyürek, 2000; Townsend and Walsh, 2001).

A top-down hierarchical classification approach was developed in this study to map forest over large mountainous terrains. The overall idea of this approach is to reduce spectral variety over areas to be mapped and to improve mapping accuracy over large mountainous areas. The approach consists of three major steps. The first step is to partition a large area into several small mapping zones (Bauer et al., 1994; Homer et al., 1997; Manis et al., 2000; Reese et al., 2002). Forest mapping is then conducted in each zone independently. At the second step, forest areas are separated from non-forest areas through a binary classification. At the third step, forested areas are then further classified into forest types by coupling Landsat imagery and two topographic variables extracted from a coarse DEM (such as DEMs derived from 1:250,000 topographic maps) which are readily available.

2.1. Spatial partitioning

The general process to partition mapping zones, which often involves analyzing some biophysical factors (such as climate, soil and vegetation) and visually interpretation of existing imagery (Albert, 1995; Manis et al., 2000), is often complex. In this study, two simple guidelines are suggested for stratifying a large mountainous region into smaller mapping zones.

First, each mapping zone should be completely contained in one scene Landsat image. Due to the temporal difference, the spectral characters of images may differ from scene to scene (Chen and Zhao, 2003). So it would be better to mapping forest within each scene.

Second, the division of each scene into different mapping zones should increase the homogeneity of solar illumination to increase

the separation power of spectral signatures. This can be achieved by dividing each scene along large rivers or major mountain ridges because solar illumination between slopes on different sides of large rivers and mountain ridges varies dramatically.

2.2. Separation of forest and non-forest areas

At this step of forest mapping, our objective was to separate forest areas from non-forest areas accurately and semi-automatically without field survey information. A hierarchical process is employed to accomplish this objective (Fig. 1). First, training data (forest/non-forest) were “sampled” based on a Gradsect sampling protocol (Austin and Heyligers, 1989) through visual interpretation of the color composite Landsat image. Second, a large number of spectral clusters were produced using an ISODATA algorithm based on five spectral indices of Landsat image: the first two principal components, the brightness index and greenness index of Tasseled-cap transformation, and a stretched normalized difference vegetation index layer (NDVI, ranged from 0 to 255). The first two principle components can carry most information of the Landsat image. The first two components (the “brightness” and “greenness” layers) of Tasseled-cap transformation can enhance the difference between forest and non-forest (Schowengerdt, 1997). The NDVI is related to the vegetation amount and it could partly remove the topographic effect (Saha et al., 2005). So the combination of these five spectral layers can not only hold the principal information of the Landsat image, but also enhance the difference between forests and non-forests. Third, each cluster was labeled as forest, non-forest or mixed cluster based on training data. And fourth, the mixed clusters, which contain both forest and non-forest pixels, were reclassified using supervised classification and/or through visually interpretation based on Landsat ETM+ image and reliable historical forest maps. Finally, forested areas were merged to form a forest mask which will limit the areas of detailed forest mapping in the next step.

2.3. Detailed forest mapping of forested areas

At this step, forested areas are further classified into detailed forest types by coupling ETM+ images with topographic information (scaled elevation and sunniness) derived from a coarse DEM under the maximum likelihood classification. Below we describe the derivation topographic information from a coarse DEM and the classification procedure.

2.3.1. Topographic data from coarse DEM

Elevation could reflect the altitudinal gradient of vegetation and slope aspect could be used to approximate differences in exposure to solar radiation, which make these two topographic variables widely used in combination with remote sensing imagery for vegetation mapping (Frank, 1988). In the absence of high quality DEM over large mountainous areas, coarse DEMs could be derived from 1:250,000 scale digital elevation contour layer. At first, a 250 m resolution DEM could be derived from the 1:250,000 scale digital elevation contour layer. Then, using the cubic convolution interpolation algorithm, the 250 m resolution DEM is interpolated to a 90 m resolution DEM, and the 90 m relation to a 30 m resolution DEM. Normally, it is not advisable to create a high resolution DEM in this fashion. However, in this case, our objective was to capture the major pattern of topographic relief and reduce the impact caused by the subtle topographic differences. We compared the coarse DEM with a high quality DEM (derived from 1:50,000 topographic maps) in Tacheng town, Weixi, the mean absolute difference is about 30 m. To decrease the effect of height error on forest mapping, a scaled elevation layer values ranging from 0 to 255, was linearly stretched from the coarse DEM. The

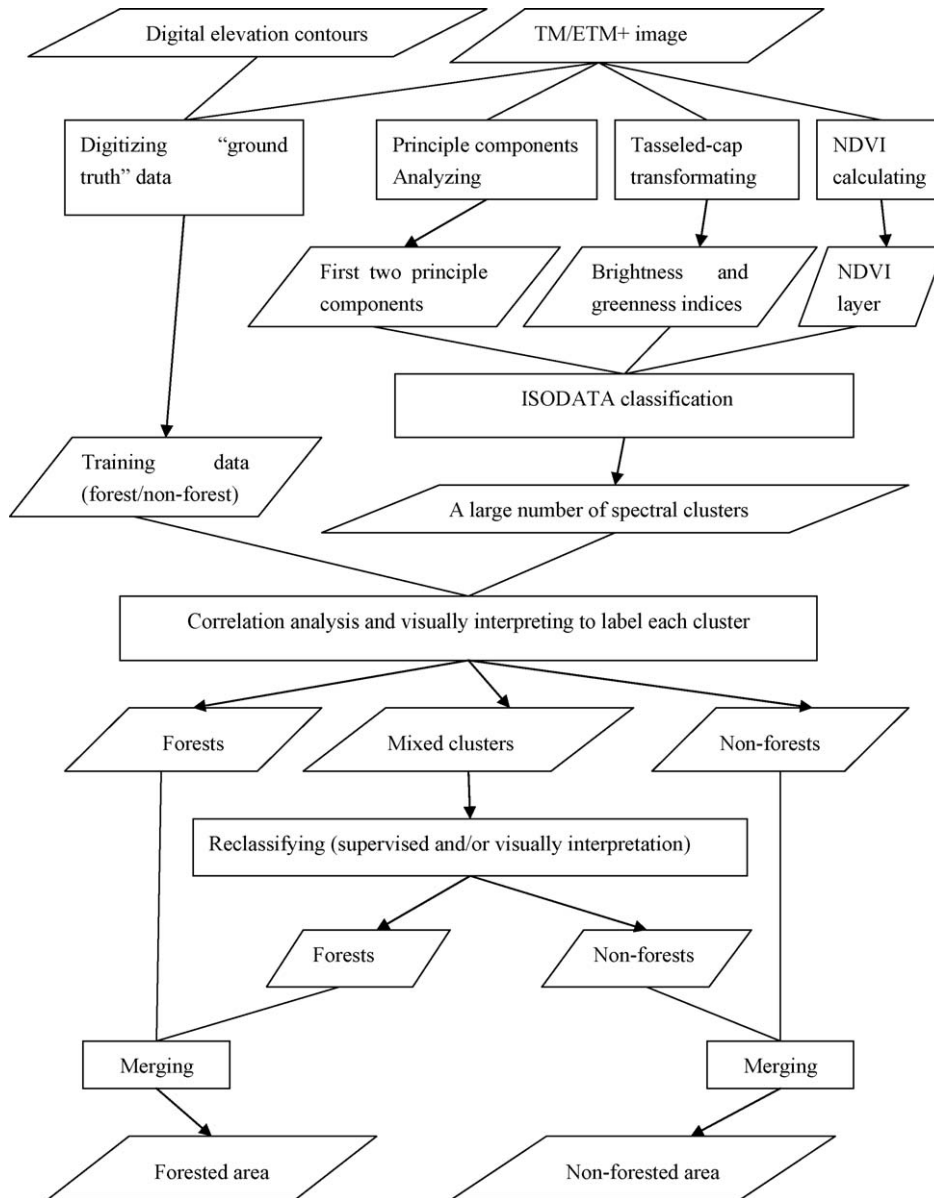


Fig. 1. Process of forest mask formation.

above process not only allows us to achieve this objective but also eliminated the need of a high quality DEM which is often difficult to obtain over areas with high relief and limited access for developing countries.

The slope aspect (measured in degree), derived from the coarse DEM, was further transformed into another variable referred to as sunniness through Eq. (1). It is subjective to make the value of sunniness ranges from 1 to 51.

$$\text{sunniness} = 25 \times \lfloor \cos(135 - \text{aspect}) \rfloor + 26 \quad (1)$$

In Eq. (1), $\lfloor x \rfloor$ is a function which makes the variable x an integer.

A total of eight variables (Landsat ETM+ bands 1–5 and 7, the scaled elevation, and the sunniness, are used for further classification of forested areas.

2.3.2. Maximum likelihood classification

Under the assumption of multi-dimensional normal distribution, a discriminant function for the forest i , was given by Eq. (2). Each pixel with the attribute vector X in the forested area would be

assigned to forest k , if $D_k(X)$ was the greatest among all the forest types.

$$D_i(X) = -\ln(|Cov_i|) - (X - M_i)^T Cov_i^{-1} (X - M_i) \quad (2)$$

where X is the attribute vector of the candidate pixel; T means to transpose the vector. M_i is the mean vector of the training data of forest i ; Cov_i is the covariance matrix of the training data of forest i and Cov_i^{-1} is the inverse matrix of Cov_i .

3. Case study

3.1. Study area

Owing to its rich biodiversity, the mountains in Southwest China is identified as a global biodiversity hotspot (Myers, 1988; Myers et al., 2000; Conservation International, 2004). As a part of this hotspot, the northwest part of Yunnan province (NW-Yunnan), also harbors at least 165 mammal species, 455 bird species and 750 endemic spermatophyte species in 15 counties covering an area of 69,000 km². Illegal hunting, overgrazing and firewood collection

Table 1
Classification scheme used for forest mapping in NW-Yunnan.

Land cover type	Description
1. Forest	Woody perennial plants covered area
1.1 Forest-fir	Forest dominated by fir (<i>Abies</i> sp.) and/or spruce (<i>Picea</i> sp.)
1.2 Forest-pine	Forest dominated by pine (<i>Pinus</i> sp.)
1.3 Forest-oak	Forest/shrub dominated by oak (<i>Quercus</i> sp.)
1.4 Broadleaved forests	Dominated by broadleaved trees such as <i>Lithocarpus</i> sp., <i>Machilus</i> sp., <i>Betula</i> sp., and <i>Quercus acutissima</i> <i>Lithocarpus</i>
2. Non-forest	Developed area (farmland, town, village), water body, talus, bare soil/sand/rock, grassland, perennial snow or ice, et al.

are some of the primary threats to biodiversity in this region (Jiao et al., 2002; Xiao et al., 2003; Yang et al., 2004). Inventory of forest cover changes is one of the important tasks to identify areas seriously impacted by these threats. Forest mapping is an important part of this inventory task.

Four counties (Shangri-La, Deqin, Weixi and Lijiang¹) in NW-Yunnan were selected as core area for a joint research project on biodiversity conservation and sustainable development between Chinese Academy of Sciences and University of Wisconsin-Madison. These four counties are located between 26°34'–29°16'N and 98°35'–100°32'E, and comprising a total area of 31,400 km². The elevation in this region ranges from about 1200 m to 6740 m above sea level. The average slope is 23°, calculated from a 30 m resolution DEM derived from 1:250,000 topographic maps. Patterns of climate and vegetation vary from subtropical to warm temperate and cold temperate (Wu and Jin, 1987). The major vegetation types include dark conifers forests, pine forests, hard leaf evergreen broadleaved forests, evergreen/deciduous broadleaved forests, mixed broadleaved and conifers forests, alpine and subalpine scrubs and meadows, and dry valley vegetation (Wu and Jin, 1987).

The whole area was partitioned into four scenes with respect to the World Referencing System-2 (<http://landsat.gsfc.nasa.gov/about/wrs.html>). Each scene was further divided into mapping zones by using the Yangtze River and the Mekong River as boundaries (Fig. 2). A total of eight mapping zones were created for this study area.

3.2. Forest classification scheme

The vegetation classification scheme used in this study was revised from the Chinese vegetation schemes (Wu, 1980). The Chinese vegetation scheme is widely used in China (Ren and Beug, 2002; Pan et al., 2003; Yu et al., 2005). Basically, we classified the whole area into forest and non-forest. Forest was further classified into conifer forest, hard leaf evergreen broadleaved forests (forest-oak), and broadleaved forest. The dark conifer forest (forest-fir) and pine forest (forest-pine) are the two dominated conifer forests in this region (Table 1).

3.3. Datasets

Four scenes of Landsat ETM+ images (Table 2) for the whole area were downloaded from the Global Land Cover Facility website (<http://glcf.umd.edu/>). These images had been orthorectified with a root mean square error less than 50 m by NASA (Tucker et al., 2004).

A 250 m resolution DEM was derived from the 1:250,000 scale digital elevation contour layer (created by the State Bureau of

Table 2
Landsat ETM+ images used in this study.

Scene-id (path-row)	132-040	132-041	131-041	131-042
Acquiring date	2000, December 25	2000, December 25	2000, December 2	2001, January 3

Surveying and Mapping, Beijing, China). Using the cubic convolution interpolation algorithm, the 250 m resolution DEM was interpolated to 90 m resolution DEM, and then to a 30 m resolution DEM (we called it the coarse DEM). In order to examine the usefulness of coarse topographic data in improving mapping accuracy, we also created a high quality DEM at 30 m resolution from 1:50,000 scale topographic maps (created by the State Bureau of Surveying and Mapping, Beijing, China) in Tacheng town, Weixi County, with a total area of 770 km² for comparison. The mean absolute difference between the coarse DEM and the high quality DEM is 29.4 m ($n = 853,634$, Fig. 3).

The sunniness layers were produced from these two DEMs by Eq. (1), respectively. Both DEMs were stretched to scaled elevation layers to obtain values ranging from 0 to 255.

Historical forest cover maps were digitized from the topographic maps (the scale = 1:50,000 or 1:100,000) which were produced based on aerial photos taken in 1960s and field surveys conducted by the Headquarters of the General Staff, Chinese People's Liberation Army in 1960s.

All these data were georeferenced to the Beijing 1954 coordinates system (Projection: Gauss-Kruger, Spheroid: Krasovsky 1940, Datum: Pulkovo 1942, Central Median: 99, False Easting: 500,000).

3.4. Training and validation data collection

We used 70% canopy closure as a threshold to define typical forests. This criterion is also used by other researchers (Mickelson et al., 1998; Reese et al., 2002). For typical non-forest area, we defined the canopy closure to be less than 10%. Validation data for forests and non-forests were collected under such criteria.

The sampling design for collecting training and validation data was of a two-level partition approach. At the first level, the whole study area was partitioned into 19 grids with the size of 20 min in latitude by 30 min in longitude. At the second level each grid was further divided into 16 primary sampling units (PSUs) of 5 min in latitude by 7.5 min in longitude. Within each grid, one PSU was selected randomly as a sampling site. Thus, our field data for detailed forest mapping satisfied the criterion of spatial distribution for sampling design (Stehman and Czaplewski, 1998).

The field data were collected along transects in each PSU to be sampled. These transects were designed to pass through a lower position in the PSU to the upper brim of forest. In addition, these transects passed both sunlit and shaded slopes. Because of the limitation of location accuracy, we identified some homogenous plots of about 3 × 3 pixels as secondary sampling units in the field as well as in the Landsat ETM+ color composite image (bands 7, 4, 2 in RGB). The distance between any two plots was greater than three pixels.

A field survey was performed throughout the whole area with an aid of a Global Position System (GPS) receiver (Garmin eTrex) for location in 2002 November (dry season) and 2004 May (wet season). We obtained 990 plots which were labeled as forests or non-forests. These plots were used as validating data to assess the accuracy of the forest mask.

Another field survey was carried out between the upper Yangtze and Mekong River from June to July in 2006. Eight PSUs were sampled in the mapping zone 13240-1 and 13241-2. We obtained 829 plots as ground-truth data in mapping zone 13240-1 and 1024 plots in 13241-2. These plots were labeled as certain

¹ The Lijiang County was partitioned into Gucheng district and Yulong County in 2003.

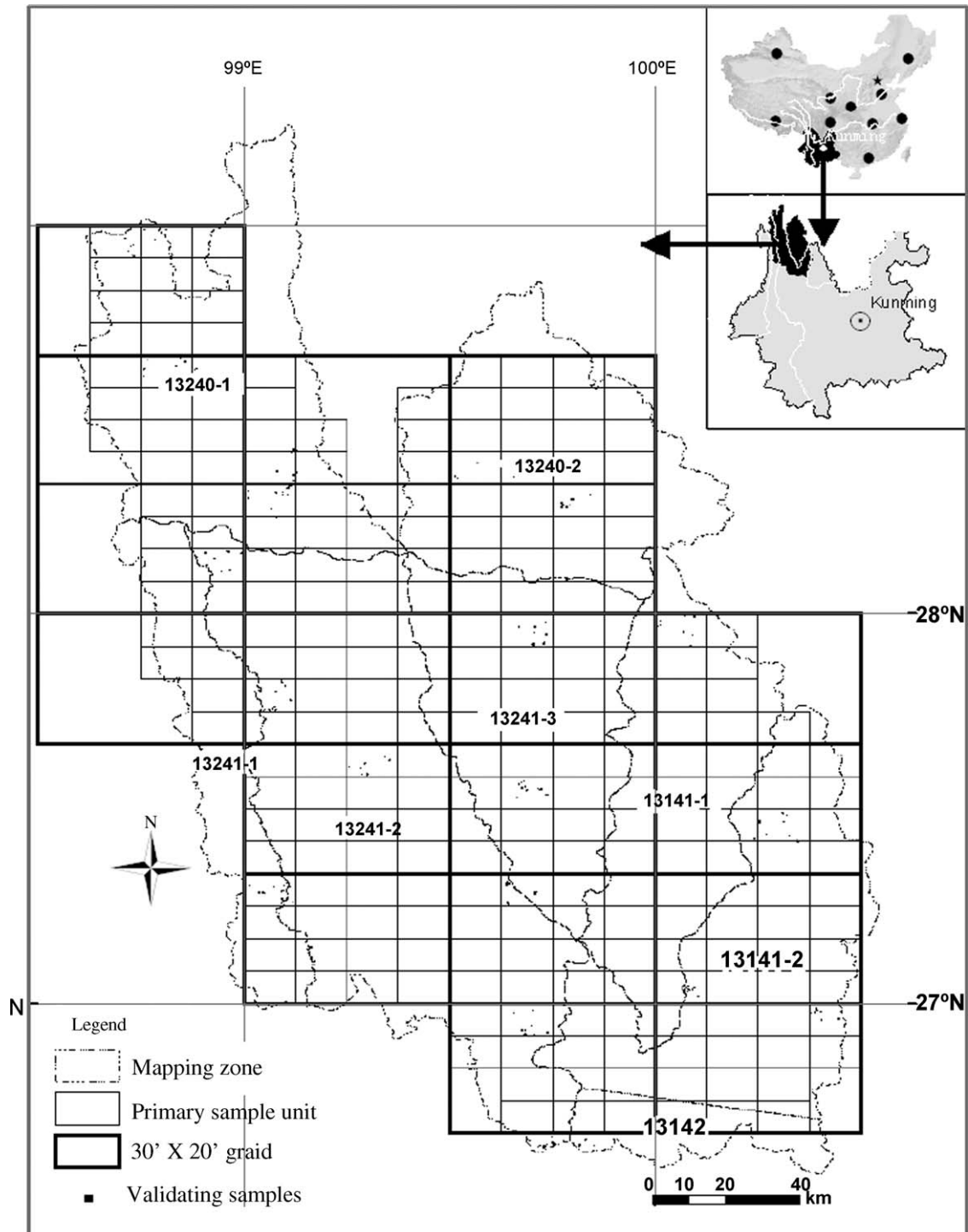


Fig. 2. Mapping zone partition and sampling design for forest mapping in NW-Yunnan.

forest types. About half of these plots were selected randomly as validating data to assess the accuracy of the forest maps we produced in the second stage, while the remainder used as training data in maximum likelihood classification, just as previous studies did (Bardossy and Samaniego, 2002; Reese et al., 2002).

3.5. Forest mapping

Forest mapping was conducted in each mapping zone separately. At the first level, a forest mask was extracted in all eight mapping zones without using field survey data. At the second

level, in order to evaluate the effectiveness of the coarse DEM in improving accuracy, detailed forest maps were produced using maximum likelihood classification based on different datasets. The whole mapping procedure was conducted under Erdas Imagine (Leica Geosystems Geospatial Imaging, LLC, Norcross, GA, US).

3.5.1. Creation of a forest mask

An ISODATA clustering was performed based on five spectral indices: the first two principle components (carrying $96 \pm 1.4\%$ information of the six bands, $n = 8$), the brightness and greenness indices of Tasseled-cap transformation (Landsat 5 TM coefficients were

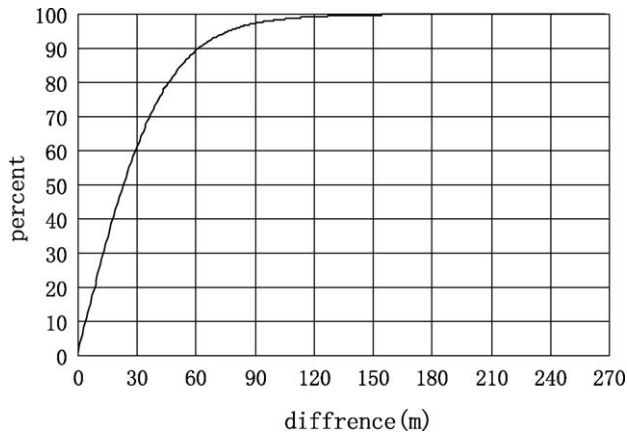


Fig. 3. The accumulated histogram of the absolute differences between the coarse DEM and the high quality DEM in Tacheng town, Weixi.

used), and the stretched NDVI layer (values ranged from 0 to 255). The maximum number of clusters is a critical parameter of ISODATA algorithm. Generally, in an ISODATA classification, the more the spectral clusters, the less the dispersion within a cluster. So a large number (typically 100–400) is often given to this parameter recently (Cihlar, 2000; Ozesmi and Bauer, 2002). However, with a larger number of clusters, more time and training data are needed to label the clusters. A trade off is needed. The relationship between the within cluster dispersion and the maximum cluster number was investigated by a series of ISODATA classification in the mapping zone 13240-1, 13241-2 and 13241-3 (Fig. 4). The within group dispersion value, defined by Wilks (1962), did not change dramatically when the cluster number ranged from 30 to 100. So we chose 60 as the maximum cluster number for all mapping zones arbitrarily.

In order to label the clusters produced from the ISODATA classification, some training data (forest and non-forest) were obtained by visual interpretation of the Landsat ETM+ color composite image (bands 7,4,2 or 4,3,2 or 4,5,3 in RGB) through a Gradsect sampling protocol (Austin and Heyligers, 1989). Eight elevation intervals were defined (elevation less than 2000 m, 2000–2500 m, 2500–3000 m, ..., 4500–5000 m, and greater than 5000 m). With the aid of digital elevation contour layer (the scale = 1:250,000), at least 40 plots of 3 × 3 pixels were selected as training data at each elevation interval on both sunlit and shaded slopes in each mapping zone.

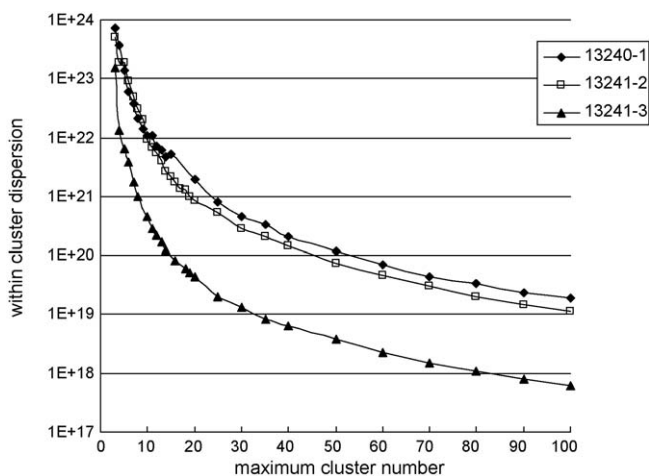


Fig. 4. Relationship between within group dispersion and maximum cluster number in ISODATA classification.

Based on the training data, 95% ($n = 8$) of spectral clusters from ISODATA classification could be labeled as forest or non-forest. Only few clusters which contained both forest and non-forest pixels were classified again using maximum likelihood classifier based on the Landsat ETM+ images. For some areas that were totally dark in the color composite images, we labeled these areas as forest only if they were forests in historical forest map and they were adjacent to forests. The whole process of creating a forest mask was showed in Fig. 1.

3.5.2. Detailed forest mapping

In the absence of high quality DEMs over large area, a primary objective of this study is to evaluate the effectiveness of coarse digital topographic data in improving accuracy of detailed forest mapping. To fulfill this objective, detailed forest maps were produced using maximum likelihood classification method based on different datasets. The method was tested in three areas: Tacheng Town, mapping zones 13240-1 and 13241-2. For the Tacheng Town, we used the four datasets: (a) Landsat ETM+ image data alone (bands 1–5 plus band 7); (b) the combination of the first two principle components, the first two components of Tasseled-cap transformation, and the stretched NDVI layer of the Landsat ETM+ image; (c) Landsat ETM+ images coupled with the two topographic data layers derived from the coarse DEM; (d) Landsat ETM+ images coupled with the two topographic data layers derived from the high quality DEM. This will allow us to evaluate the effectiveness of the use of topographic information derived from the coarser DEM. For the two mapping zones, we only used datasets (a–c). This will allow us to assess the stability of our overall approach when applying to other areas.

3.5.3. Accuracy assessment and statistic test

An error matrix could be used to calculate the overall accuracy, Khat value, producer's accuracy, and user's accuracy (Stehman, 1997; Congalton and Green, 1999; Lillesand et al., 2007). A binomial test (applying normal approximation with test statistic Z) was used to examine the differences of accuracies between any two detailed forest maps produced above. Suppose the overall accuracies of two maps were P_1 and P_2 , which were calculated based on the same reference data of size N , a test of $H_0, P_1 \geq P_2$, is obtained from Eq. (3).

$$Z = \frac{P_1 - P_2}{\sqrt{(P_1(1 - P_1) + P_2(1 - P_2))/N}} \quad (3)$$

In Eq. (3), Z is distributed as a standard normal random variable.

4. Results

4.1. Accuracy of forest versus non-forest map

The 990 plots, which were labeled as forest or non-forest, were used as ground truth data for assessing the accuracy of the forest versus non-forest map (Fig. 5). The overall accuracy is 0.97 and Khat value is 0.94 of whole area ($n = 10,776$, Table 3). This suggests that the forest mask is of high accuracy.

4.2. Accuracy of detailed forest maps

Table 4 shows the overall accuracies and Khat values of detailed forest maps produced based on different datasets. Tables 5 and 6 are the error matrices of detailed forest maps produced based on Landsat ETM+ images and coarse topographic data in mapping zone 13240-1 and 13241-2.

Compared with mapping based on Landsat ETM+ images alone, using topographic data derived from coarse DEMs could increase

Table 3
Mapping accuracy of forest versus non-forest in all the subregions.

Scene-id	13240		13241			13141		13142	WA ^a
Zone	1	2	1	2	3	1	2		
OA ^b	0.96	0.97	1.00	0.97	0.97	0.98	0.96	0.97	0.97
Khat	0.91	0.94	0.99	0.93	0.93	0.96	0.91	0.94	0.94
n ^c	1389	867	1581	3177	1213	471	1164	914	10,776

^a The Whole Study Area.
^b Overall accuracy.
^c Pixel number of validation data.

the overall accuracies (from 0.76 to 0.89 in mapping zone 13241-2, $Z = 9.877$, $p = 0.000$, $n = 1618$; and from 0.78 to 0.84 in mapping zone 13240-1, $Z = 3.740$, $p = 0.000$, $n = 1189$). The producer's accuracies for all the forest types in both mapping zones were also increased significantly. These results suggest that our approach is effective in increasing the accuracy of forest mapping over rugged terrains.

From the test of Tacheng town, using high quality topographic data instead of coarse topographic data in the classification procedure, the increase in the overall accuracy was not significant ($Z = 0.964$, $p = 0.168$, $n = 592$), and the increase in the producer's accuracy was not significant for each forest type, either. These results suggest that the coarse topographic information is useful in increasing the accuracy of forest mapping over rugged terrain areas in the absence of high quality DEMs.

Although the five spectral indices could enhance the differences between forests and non-forests, detailed forest mapping based on the combination of these spectral indices were not better than mapping based on the Landsat alone.

Table 4
The overall accuracies of detailed forest maps over the three test areas, produced from a maximum likelihood classification, based on different datasets. Better results appeared when the two topographic variables were used.

Dataset ^a	Tacheng (n = 592)		13241-2 (n = 1618)		13240-1 (n = 1189)	
	OA ^b	Khat	OA	Khat	OA	Khat
1–5, 7	0.74	0.56	0.76	0.63	0.78	0.58
$P_1, P_2, T_1, T_2, NDVI$	0.68	0.48	0.74	0.59	0.74	0.57
1–5, 7, E_c, S_c	0.84	0.72	0.89	0.83	0.84	0.74
1–5, 7, E_h, S_h	0.86	0.75	–	–	–	–

^a 1–5, 7 represent bands 1–5 and band 7 of Landsat ETM+ image; P_1, P_2, T_1, T_2 , and NDVI, represent the first two principle components, the first two components of Tasseled-cap transformation, and the stretched NDVI layer of the Landsat ETM+ image, respectively. E_c, S_c and E_h and S_h represent the scaled elevation and sunniness layers derived from the coarse DEM and the high quality DEM, respectively.
^b Overall accuracy.

Table 5
Error matrix of detailed forest map in zone 13240-1 produced based on Landsat ETM+ image combined with coarse topographic layers.

	Validating data (n = 1189)			
	Fir	Oak	Pine	User's Acc.
Forest-fir	551	4	8	0.98
Forest-oak	50	333	36	0.79
Forest-pine	37	50	120	0.58
Producer's accuracy	0.86	0.86	0.73	
Overall accuracy	0.84			
Khat	0.74			

Table 6
Error matrix of detailed forest map in zone 13241-2 produced based on Landsat ETM+ image combined with coarse topographic layers.

	Validating data (n = 1618)			
	Fir	Oak	Bro. F	User's Acc.
Forest-fir	674	5	5	0.99
Forest-pine	29	632	37	0.91
Broadleaved forest	19	75	142	0.60
Producer's accuracy	0.93	0.89	0.77	
Overall accuracy	0.89			
Khat	0.83			

5. Discussion and summary

5.1. The improvement in both accuracy and efficiency to categorize forest versus non-forest

Although forest versus non-forest map can be extracted automatically or semi-automatically from Landsat imagery over some mountainous terrains, the primary means to do this is still

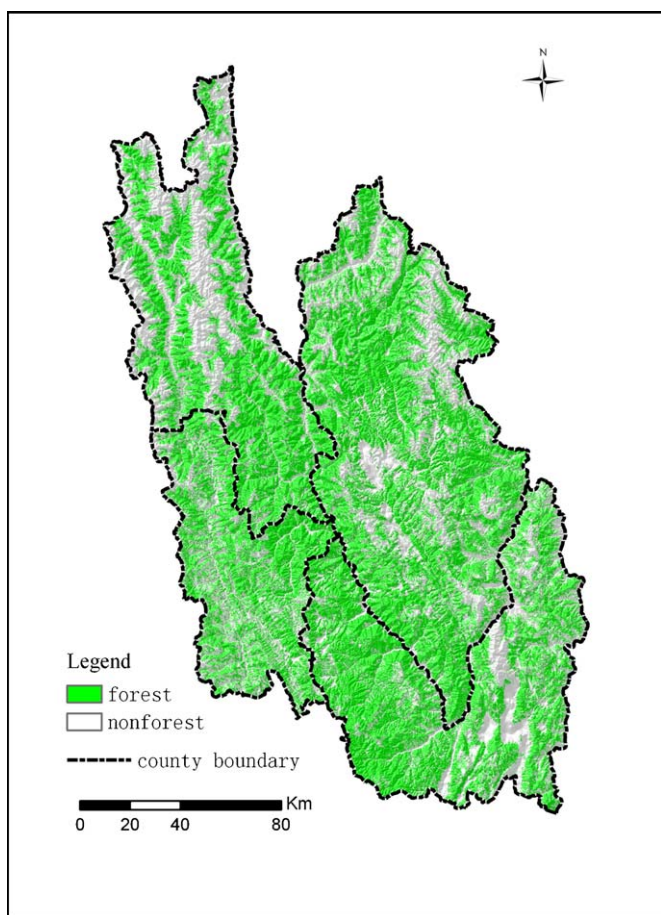


Fig. 5. Forest cover of the four counties in NW-Yunnan in the early 2000s.

visual interpretation of satellite imagery in the very rugged areas such as Northwest Yunnan, China (Xiao et al., 2003; Jiang et al., 2004; Liu et al., 2006). This manual mapping process is very tedious and time-consuming. Furthermore, the visual interpretation process is very difficult, if not impossible, to be repeated over a large area. Using the conventional digital classification methods, training data from field survey are often needed. However, collecting ground-truth data is also a tough and cost-consuming task in mapping forest and non-forest over steep mountainous terrains. In this study, it only took 10 person-days to map forests versus non-forests over these four counties (the total area is 31,400 km²).

The overall accuracy of whole area is 0.970 even without using field survey data as training data. The results indicate our forest versus non-forest maps in all mapping zones are of high quality, even compared to some successful practices, such as Tokola et al. (2001), Dorren et al. (2003), Sivanpillai et al. (2005) and Kozak et al. (2007).

5.2. Efforts to improve detailed forest mapping

Mapping forest from satellite imagery over the steep mountainous terrain remains to be a challenge (Leprieur et al., 1988; Tokola et al., 2001; Dorren et al., 2003). We attempted to overcome the challenge by using a hierarchical approach and with the addition of two topographic variables derived from small scale digital elevation layer.

As the results indicate, even the topographic data derived from the coarse DEMs could be used to improve accuracies of detailed forest mapping. This could be explained by the fact that pixels of different forest types often occupy different topographic locations even they might have the same spectral respond (Dorren et al., 2003; Lillesand et al., 2007). Meanwhile, coupled with coarse topographic data in the mapping procedure could achieve almost the similar accuracy as coupled with the high quality topographic data did in the Tacheng case. One possible reason might be that the forest scheme used in this study is too broad. Given more detailed forest types for special purpose to be mapped, using the high quality DEM as additional input might be better. The study area is so rugged that the 1:50,000 topographic maps created in 1960s might not be very precise. The height error of the “high quality DEM” might be close to that of the coarse DEM, which caused the similar performance of both DEMs in detailed forest mapping.

In the absence of high quality DEMs, our results suggest that DEMs derived from 1:250,000 topographic maps could also used to improve detailed forest mapping accuracy in very rugged areas like Northwest Yunnan.

5.3. Summary

As it was shown in the case study, using this hierarchical approach, forest and non-forest could be separated by a semi-automatic process over steep mountainous terrain without field survey data as training data. Furthermore, in the absence of high quality DEM, topographic data derived from 1:250,000 digital elevation contour layer can be incorporated with Landsat ETM+ imagery to improve accuracy of detailed forest mapping. In conclusion, the new approach devised in this study is effective in forest mapping over very rugged terrains, such as Northwest Yunnan, China.

Acknowledgements

Funding from International Partnership Project “Human Activities and Ecosystem Changes” of Chinese Academy of Sciences (No. CXTD-Z2005-1), ‘Hundred Talents’ Program of Chinese Academy of Sciences, the field forefront program of LREIS and

the NSF IGERT grant awarded to the University of Wisconsin-Madison is greatly appreciated. This study was also supported by TNC and the Chinese Academy of Sciences (Grant No. KSCX2-1-09). We would like to thank Professor Qikun Zhao for his helpful suggestions for this study. Rongxun Wang, Jian Liu and Feihua Yang (PHD candidates in University of Wisconsin-Madison) gave very useful comments on this study. We are also grateful to the local residents, the local forestry bureaus, local governments in north-west Yunnan, the forestry department of Yunnan province for their support in our field work. Special thanks are giving to Mr. Chunxiang Chen for his selfless help. We also would like to thank the anonymous reviewer for the very helpful comments and generous suggestions.

References

- Albert, D.A., 1995. Regional Landscape Ecosystems of Michigan, Minnesota, and Wisconsin: A Working Map and Classification (Fourth revision: July 1994). U.S. Department of Agriculture, Forest Service, North Central Forest Experiment Station, General Technical Report, NC-178.
- Anderson, J.R., Hardy, E.E., Roach, J.T., Witmer, R.E., 1976. A land use and land cover classification system for use with remote sensor data, US Geological Survey Professional Paper 964, 28 pp.
- Austin, M.P., Heyligers, P.C., 1989. Vegetation survey design for conservation: Gradsect sampling of forests in North-eastern New South Wales. *Biological Conservation* 50, 13–32.
- Avci, M., Akyürek, Z., 2000. A hierarchical classification of Landsat TM imagery for landcover mapping. Thesis of Master degree, Middle East Technical University.
- Bardossy, A., Samaniego, L., 2002. Fuzzy rule-based classification of remotely sensed imagery. *IEEE Transactions on Geoscience and Remote Sensing* 40, 362–374.
- Bauer, M.E., Burk, T.E., Ek, A.R., Coppin, P.R., Lime, S.D., Walsh, T.A., Walters, D.K., Befort, W., Heinzen, D.F., 1994. Satellite inventory of Minnesota forest resources. *Photogrammetric Engineering and Remote Sensing* 60, 287–298.
- Blesius, L., Weirich, F., 2005. The use of the minnaert correction for land-cover classification in mountainous terrain. *International Journal of Remote Sensing* 26, 3831–3851.
- Bossard, M., Feranec, J., Otahel, J., European Environment, A., 2000. CORINE Land Cover Technical Guide: Addendum 2000. European Environment Agency.
- Chen, D.M., Zhao, Y.S., 2003. Interpreting and processing of remote sensing imagery. In: Zhao, Y.S. (Ed.), *Analysis Principles and Methods of Remote Sensing Application*. Science Press, Beijing, (in Chinese), pp. 166–210.
- Cihlar, J., 2000. Land cover mapping of large areas from satellites: status and research priorities. *International Journal of Remote Sensing* 21, 1093–1114.
- Congalton, R.G., Green, K., 1999. *Assessing the Accuracy of Remotely Sensed Data: Principles and Practices*. Lewis Publications, Boca Raton, FL.
- Conservation International, 2004. Hotspots Revisited. In: *Conservation International*, Washington, DC, USA. <http://www.biodiversityhotspots.org/xp/Hotspots/resources/maps.xml>. (website last visited in April 3, 2007).
- Dorren, L.K.A., Maier, B., Seijmonsbergen, A.C., 2003. Improved Landsat-based forest mapping in steep mountainous terrain using object-based classification. *Forest Ecology Management* 183, 31–46.
- Fahsi, A., Tsegaye, T., Tadesse, W., Coleman, T., 2000. Incorporation of digital elevation models with Landsat-TM data to improve land cover classification accuracy. *Forest Ecology Management* 128, 57–64.
- Frank, T., 1988. Mapping dominant vegetation communities in the Colorado Rocky Mountain Front Range with Landsat Thematic Mapper and digital terrain data. *Photogrammetric Engineering and Remote Sensing* 54, 1727–1734.
- Franklin, S.E., Wilson, B.A., 1992. A three-stage classifier for remote sensing of mountain environments. *Photogrammetric Engineering and Remote Sensing* 58, 449–454.
- Homer, C.G., Ramsey, R.D., Edwards, T.C., Falconer, A., 1997. Landscape cover-type modeling using a multi-scene thematic mapper mosaic. *Photogrammetric Engineering and Remote Sensing* 63, 59–67.
- Jiang, X.B., Zhou, Q.G., Li, A.N., 2004. Landscape pattern of Diqing, Yunnan. *Journal of Mountain Research* 22, 164–168 (in Chinese with English abstract).
- Jiao, Y.M., Wang, J.L., Ma, J., 2002. Analysis of landuse/landcover changing factors in the Three-Parallel-River Region. *Journal of Yunnan Normal University (Natural Sciences Edition)* 22, 59–65 (in Chinese with English abstract).
- Kozak, J., Estreguil, C., Vogt, P., 2007. Forest cover and pattern changes in the Carpathians over the last decades. *European Journal of Forest Research* 126, 77–90.
- Kushwaha, S.P.S., Hazarika, R., 2004. Assessment of habitat loss in Kameng and Sonitpur Elephant Reserves. *Current Science* 87, 1447–1453.
- Leprieur, C.E., Durand, J.M., Peyron, J.L., 1988. Influence of topography on forest reflectance using Landsat-TM and digital terrain data. *Photogrammetric Engineering and Remote Sensing* 54, 491–496.
- Lillesand, T.M., Kiefer, R.W., Chipman, J.W., 2007. *Remote Sensing and Image Interpretation*, 6th edition. John Wiley & Sons, Hoboken, NJ.
- Liu, M.L., Qi, Q.W., Zou, X.P., Li, J., 2006. Spatial-temporal changes of land use/cover in border areas of Yunnan Province. *Remote Sensing for Land and Resource* 1, 75–78 (in Chinese with English abstract).

- Manis, G., Homer, C., Ramsey, R.D., Lowry, J., Sajwaj, T., Graves, S., 2000. The development of mapping zones to assist in land cover mapping over large geographic areas: a case study of the Southwest ReGAP Project. *GAP Analysis Bulletin*, 9. U.S. Geological Survey, pp. 13–16.
- Mickelson, J.G., Civco, D.L., Silander, J.A., 1998. Delineating forest canopy species in the northeastern United States using multi-temporal TM imagery. *Photogrammetric Engineering and Remote Sensing* 64, 891–904.
- Myers, N., 1988. Threatened biotas: hotspots in tropical forests. *The Environmentalist* 8, 178–208.
- Myers, N., Mittermeier, R.A., Mittermeier, C.G., da Fonseca, G.A.B., Kent, J., 2000. Biodiversity hotspots for conservation priorities. *Nature* 403, 853–858.
- Olthof, I., Fraser, R.H., 2007. Mapping northern land cover fractions using Landsat ETM+. *Remote Sensing of Environment* 107, 496–509.
- Osborne, P.E., Alonso, J.C., Bryant, R.G., 2001. Modelling landscape-scale habitat use using GIS and remote sensing: a case study with great bustards. *Journal of Applied Ecology* 38, 458–471.
- Ozesmi, S.L., Bauer, M.E., 2002. Satellite remote sensing of wetlands. *Wetlands Ecology and Management* 10, 381–402.
- Pan, Y., Li, X., Gong, P., He, C., Shi, P., Pu, R., 2003. An integrative classification of vegetation in China based on NOAA AVHRR and vegetation–climate indices of the Holdridge life zone. *International Journal of Remote Sensing* 24, 1009–1027.
- Paul, F., Huggel, C., Kaab, A., 2004. Combining satellite multispectral image data and a digital elevation model for mapping debris-covered glaciers. *Remote Sensing of Environment* 89, 510–518.
- Reese, H.M., Lillesand, T.M., Nagel, D.E., Stewart, J.S., Goldmann, R.A., Simmons, T.E., Chipman, J.W., Tessar, P.A., 2002. Statewide land cover derived from multi-seasonal Landsat TM data: a retrospective of the WISCLAND project. *Remote Sensing of Environment* 82, 224–237.
- Ren, G.Y., Beug, H.J., 2002. Mapping Holocene pollen data and vegetation of China. *Quaternary Science Reviews* 21, 1395–1422.
- Richter, R., 1998. Correction of satellite imagery over mountainous terrain. *Applied Optics* 37, 4004–4015.
- Saha, A.K., Arora, M.K., Csaplovics, E., Gupta, R.P., 2005. Land cover classification using IRS LISS III image and DEM in a rugged terrain: a case study in Himalayas. *Geocarto International* 20, 33–40.
- Schowengerdt, R.A., 1997. *Remote sensing: models and methods for image processing*. Academic Press, San Diego.
- Sivanpillai, R., Smith, C.T., Srinivasan, R., Messina, M.G., Ben Wu, X., 2005. Estimating regional forest cover in East Texas using enhanced thematic mapper (ETM plus) data. *Forest Ecology Management* 218, 342–352.
- Skidmore, A.K., Gauld, A., Walker, P., 1996. Classification of kangaroo habitat distribution using three GIS models. *International Journal of Geographical Information Science* 10, 441–454.
- Stehman, S.V., 1997. Selecting and interpreting measures of thematic classification accuracy. *Remote Sensing of Environment* 62, 77–89.
- Stehman, S.V., Czaplewski, R.L., 1998. Design and analysis for thematic map accuracy assessment: fundamental principles. *Remote Sensing of Environment* 64, 331–344.
- Tokola, T., Sarkeala, J., Van der Linden, M., 2001. Use of topographic correction in Landsat TM-based forest interpretation in Nepal. *International Journal of Remote Sensing* 22, 551–563.
- Townsend, P.A., Walsh, S.J., 2001. Remote sensing of forested wetlands: application of multitemporal and multispectral satellite imagery to determine plant community composition and structure in southeastern USA. *Plant Ecology* 157, 129–149.
- Tucker, C.J., Grant, D.M., Dykstra, J.D., 2004. NASA's Global Orthorectified Landsat Data Set. *Photogrammetric Engineering and Remote Sensing* 70, 313–322.
- Wechsler, S.P., 2003. Perceptions of Digital Elevation Model Uncertainty by DEM Users. *URISA Journal* 15, 57–64.
- Wilks, S., 1962. *Mathematical Statistics*. Wiley and Sons, New York.
- Wu, Z.Y., 1980. *Chinese Vegetation*. Science Press, Beijing, in Chinese.
- Wu, Z.Y., Jin, Z.Z., 1987. The flora of Yunnan vegetation. In: Wu, Z.Y., Zhu, Y.C., Jiang, H.Q. (Eds.), *The Vegetation of Yunnan*. Science Press, Beijing, (in Chinese), p. 37.
- Wulder, M.A., Dechka, J.A., Gillis, M.A., Luther, J.E., Hall, R.J., Beaudoin, A., 2003. Operational mapping of the land cover of the forested area of Canada with Landsat data: EOSD land cover program. *Forestry Chronicle* 79, 1075–1083.
- Xiao, W., Ding, W., Cui, L.W., Zhou, R.L., Zhao, Q.K., 2003. Habitat degradation of *Rhinopithecus bieti* in Yunnan, China. *International Journal of Primatology* 24, 389–398.
- Yang, Y., Tian, K., Hao, J., Pei, S., Yang, Y., 2004. Biodiversity and biodiversity conservation in Yunnan China. *Biodiversity and Conservation* 13, 813–826.
- Yu, F., Li, X.-B., Wang, H., Yu, H.-J., Chen, Y.-H., 2005. Land cover classification in China based on the NDVI-Ts feature space. *Acta Phytocologica Sinica* 29, 933–944.
- Zemek, F., Herman, M., Maskova, Z., Kvet, J., 2005. Multifunctional land use—a chance of resettling abandoned landscapes? (A case study of the Zhuri territory Czech Republic). *Ekologia (Bratislava)* 24, 96–108.
- Zhu, Z.L., Waller, E., 2003. Global forest cover mapping for the United Nations Food and Agriculture Organization Forest Resources Assessment 2000 program. *Forest Science* 49, 369–380.